NASA Technical Memorandum 81745

Low and High Speed Propellers for General Aviation – Performance Potential and Recent Wind Tunnel Test Results

Robert J. Jeracki and Glenn A. Mitchell
Lewis Research Center
Cleveland, Ohio

Prepared for the
National Business Aircraft Meeting
sponsored by the Society of Automotive Engineers
Wichita, Kansas, April 7-10, 1981

NASA

LOW AND HIGH SPEED PROPELLERS FOR GENERAL AVIATION - PERFORMANCE POTENTIAL AND RECENT WIND TUNNEL TEST RESULTS

by Robert J. Jeracki and Glenn A. Mitchell

National Aeronautics and Space Administration
Lewis Research Center
Cleveland, Ohio 44135

THE VAST MAJORITY OF GENERAL-AVIATION AIRCRAFT manufactured in the United States are propeller powered. Most of these aircraft use propeller designs based on technology that has not changed significantly since the 1940's and early 1950's. This older technology has been adequate; however, with the current world energy shortage and the possibility of more stringent noise regulations, improved technology is needed. Studies conducted by NASA and industry indicate that there are a number of improvements in the technology of general-aviation (G.A.) propellers that could lead to significant energy savings. New concepts like blade sweep, proplets, and composite materials, along with advanced analysis techniques have the potential for improving the performance and lowering the noise of future propeller-powererd aircraft that cruise at lower speeds. Current propeller-powered general-aviation aircraft are limited by propeller compressibility losses and limited power output of current engines to maximum cruise speeds below Mach 0.6. The technology being developed as part of NASA's Advanced Turboprop Project offers the potential of extending this limit to at least Mach 0.8. At these higher cruise speeds, advanced turboprop propulsion has the potential of large energy savings compared with aircraft powered by advanced turbofan systems. A present-day low speed G.A. airplane and a model of a possible high speed turboprop powered airplane are shown in Fig. 1.

PROPELLER PROPULSION SYSTEM POTENTIAL

A comparison of the installed cruise efficiency of turboprop-powered and turbofan-powered propulsion systems is shown in Fig. 2 for a range of cruise speeds. The installation losses included with the propeller-powered systems are nacelle drag and with the turbofan-powered systems the losses include fan cowling external drag and the internal fan airflow losses associated with inlet recovery and nozzle efficiency. The installed efficiency available with current technology turboprop-powered general-aviation aircraft is

Jeracki and Mitchell

*Numbers in parentheses designate References at end of paper.

about 80% at speeds up to about Mach 0.5. Above this speed efficiency falls off significantly because of large propeller compressibility losses. These propellers are generally designed with blades of thickness to chord ratios (at 75% radius) that range from about 5 to 7%.

These rather thick blades, when operated at relatively high tip helical Mach numbers, are the main cause of these losses. With reciprocating powered G.A. propulsion systems the level of installed efficiency would be slightly lower than 80% due to larger nacelle (sizes) and drag and internal cooling airflow losses (1, p. 321)*.

Advanced G.A. turboprops can potentially achieve significant gains over current propellers with projected, installed cruise efficiencies of about 87% up to speeds approaching Mach 0.6. A study of advanced G.A. propeller technology (1, pp. 327-343 and 2) has indicated that these gains may be realized by utilizing composites, improved analysis methods, and a number of advanced aerodynamic concepts.

The advanced, high-speed turboprop shown in Fig. 2 is a new propulsion concept that has the potential of eliminating or minimizing compressibility losses at flight speeds to Mach 0.8. The level of potential installed efficiency projected for the advanced turboprop is considerably higher than that available with comparable technology high-bypass turbofan systems. At Mach 0.8 the installed efficiency of turbofan systems would be approximately 65% compared with about 75% for the advanced turboprop.

Under contract to NASA Lewis Research Center, McCauley Accessory Division of Cessna Aircraft Company has conducted a study to evaluate the impact of advanced propeller technologies appropriate for lower speed G.A. aircraft (1, pp. 327-343 and 2). The study identified applicable advanced technologies and assessed their potential costs and benefits. Some of the advanced technology concepts included in the study are shown in Fig. 3. This figure illustrates a thin, swept, low activity factor, composite propeller having advanced aero/acoustic airfoil sections, swept blades, and NASA proplets on the blade tips. In addition, the airfoil section shapes are carried into the hub for improved blade/spinner integration and the overall de-

sign was evolved by improving the integration of the propeller and nacelle.

The potential benefits of these advanced technologies were assessed by McCauley in a mission analysis study of several G.A. aircraft encompassing both single and twin engine aircraft ranging in cruise speed from 120 to 295 knots. In addressing the mission analysis, the aircraft were resized to take full advantage of the advanced technology benefits. Payload, range, speed, and aircraft lift to drag ratio were kept constant, and a 2 hour cruise mission was assumed. The potential trip fuel savings are shown in Fig. 4. The gains shown were obtained by comparing the advanced propeller aircraft with baseline propeller aircraft; both meeting FAR part 36 noise limits. The data points in Fig. 4 show the results of the mission analysis calculations for each aircraft while the faired curve indicates the more likely average potential gain. The application of advanced technology to lower speed G.A. propellers has the potential benefit of reducing trip fuel consumed by about 10 to 15%. The larger, higher cruise speed aircraft have the larger improvements due to the higher fuel to gross weight fraction and higher predicted propeller performance gains for these aircraft.

A model of an advanced high speed turboprop propulsion system is shown in Fig. 5. The advanced propeller would be powered by a modern turboshaft engine and gear box to provide the maximum power to the propeller with a minimum engine fuel consumption. Propeller efficiency would be kept high by minimizing or eliminating compressibility losses. This would be accomplished by utilizing thin swept blades that would be integrally designed with an area ruled spinner and nacelle. Blade sweep would also be used to reduce noise during both take-off/landing and during high speed cruise flight (3 to 5). Aircraft operations at high altitudes and Mach 0.6 to 0.8 requires much higher power than used on current propeller aircraft. A power loading (shaft horsepower divided by propeller diameter squared) about five times higher than current business turboprops would be needed to minimize propeller diameter and weight. Eight or ten blades are required to increase ideal efficiency at these higher disk loadings. In addition to these advanced concepts, a modern blade fabrication technique is needed to con-

struct the thin, highly swept and twisted blades.

A number of studies have been conducted by both NASA and industry to evaluate the potential of advanced high speed turboprop propulsion for both civil and military applications. Numerous references to specific studies and summary results are listed in Ref. (5). The trip fuel savings trend shown in Fig. 6 plotted versus operating range is a summary of these studies. Installed efficiency levels similar to those shown in Fig. 2 for comparable technology advanced turboprops and turbofans were used in most of these studies. As shown in Fig. 6, trip fuel savings is dependent on aircraft cruise speed and range.

At the bottom of the band, associated with Mach 0.8 cruise, fuel savings range from about 15 to 30% for advanced turoprop aircraft compared to equivalent technology turbofan aircraft. The larger fuel savings occurs at the shorter operating ranges where the mission is climb and descent dominated. Because of the lower operating speeds encountered during climb and descent, turboprops have an even larger performance advantage than the advantage at Mach 0.8 cruise conditions. In a similar manner, a larger fuel savings is possible at Mach 0.7 cruise (represented by the top of the band in Fig. 6). At this lower cruise speed fuel savings range from about 25 to near 40%. These fuel savings were all for advanced single rotation turboprops. A study that included co-axial counter-rotation turboprops (6) has shown that there is an additional 5 to 6% trip fuel savings at Mach 0.8 over these single rotation systems. With 2 dollar per gallon fuel, a Mach 0.7 advanced single rotation turboprop can reduce total operating cost by 20% over a comparable high bypass ratio turbofan (7).

LOW SPEED PROPELLER TESTS

As part of a program to evaluate the capability of current G.A. propeller aerodynamic and acoustic analytical prediction methods, a wind tunnel test of several G.A. propeller models were conducted in the NASA Lewis 10-by-10 foot wind tunnel. A photograph of one of these 1.524-meter (5 ft) diameter models is shown in Fig. 7 installed on the Lewis 746 kW (1000 hp) propeller test rig (PTR). Power for this PTR is provided by a 15.0 cm

(5.9 in.) diameter air turbine using a continuous flow $3.1 \times 10^6 N/m^2$ (450 psi) air system routed through the support strut. Propeller aerodynamic performance was determined using a rotating balance that measured both axial force and torque. The balance was located just downstream of the propeller models inside the nacelle. The nacelle that was tested (Fig. 7) was an axi-symmetric model of the Rockwell Turbocommander 690B shown in Fig. 1(a). The model and full-scale nacelle both had approximately the same cross sectional area distribution (relative to propeller diameter). To account for the aerodynamic interaction between the metric propeller models and the non-metric nacelle, the pressure force on the nacelle was determined based on pressure integration. The increase in nacelle drag with an operating propeller model (compared to the propeller removed case) was used to reduce the measured propeller (apparent) efficiency to obtain a net efficiency using the well established method of Ref. (8). A small efficiency correction was also made to account for the interference between the propeller flow field and the tunnel wall boundary based on the method of Refs. (9 and 10), and some detailed wall pressure measurements.

Four 3-blade propeller models were tested. These models are representative of current technology G.A. turboprop propellers designed for cruise near Mach 0.5. Representative characteristics of the four models are shown in table I. Activity factor (AF) per blade varied from 83 to 132 and thickness to chord ratio at 75% radius varied from about 5 to 9%. Two of the models incorporated airfoil technology from the World War II era and the other two used more modern airfoil technology (ARA-D from Ref. (11), and GAW-2) The three important operating conditions that were investigated are shown in table II. Cruise data was obtained at Mach 0.35 rather than the higher Mach 0.5 cruise speed of the 690B aircraft due to wind tunnel limitations. However, advance ratio and power coefficient were held to the actual aircraft values.

Typical test results from the AF = 101, NACA 16 airfoil design are shown in Fig. 8 at Mach 0.35. The data are presented in the conventional propeller performance plot format. Net thrust efficiency and a dimensionless power coefficient are plotted as ordinates. The abscissa is advance ratio which is proportion-

al to the ratio of flight or advance speed to blade tip speed. As tip speed increases from windmill (no power), the advance ratio decreases and power coefficient increases. Blade angle is set and data are taken from windmill to higher power shown by the data symbols on the power coefficient plot. The blade angle ($\beta_{3/4}$), measured at 3/4 of the propeller radius, becomes 90° when the chord of that airfoil section is aligned directly with the flight direction. As power is increased the thrust increases and, as seen in the upper data curves, the net thrust efficiency increases, reaches a peak, and then begins to drop off. All blade angles yield similar power and efficiency curves. Power loading (P/D^2) can be written in terms of propeller coefficients and free-stream conditions as:

$$\frac{P}{D^2} = \frac{C_p}{J^3} (\rho_o V_o^3)$$

From this relationship a line of constant power loading has been added to Fig. 8 and represents the design loading parameter C_p/J^3 (=0.02727) corresponding to the cruise design operating condition of J=2.234, and C_p=0.304. This line represents the design power at different propeller tip speeds. The efficiency at the design power can be found for each blade angle by locating the intersection of the design power loading line with the C_p vs J data curve for each blade angle, moving vertically up to the net efficiency curve (keeping the same J), and reading the efficiency. The design point efficiency (at design power loading and design J) can be determined by interpolation from the resulting efficiencies obtained for each blade angle. The design efficiency for the three operating conditions of table II were determined using the method described above for each of the four propellers. These conditions are takeoff, climb and cruise.

A comparison of the design point performance of the four propellers is shown in Fig. 9 at the three design conditions. Only very limited data could be taken on the AF=96, GAW-2 airfoil model and the AF=132, NACA 65 airfoil model due to the difficulty in obtaining good dynamic balance with these models. An extreme extrapolation would have been required

for the second of those models at take-off so it is not shown. The extrapolation was less severe for the other model, therefore, the takeoff efficiency is included. Analytical performance predictions based on strip integration methods similar to the established approach of Refs. (12 to 14) are plotted as line segments identified with solid symbols corresponding to the propeller configuration.

At take-off the advanced airfoil (ARA-D) appears to improve the performance over the other two models. (The high activity factor model, AF=132, not shown would be predicted to have high takeoff performance. Though the data was not near enough to the design conditions to reliably extrapolate, the measured performance at a higher advance ratio was above the other three models and would be expected to perform equal to or better than the ARA-D blades at the lower advance ratio design takeoff conditions. Both the advanced airfoil (ARA-D) and the high activity factor (AF=132) propellers appear slightly better at the climb condition than the other two models. At cruise conditions the two models with the lower AF's and the more modern airfoil technology performed slightly higher than the other models.

In general, the current G.A. analytical prediction methods tend to fairly accurately estimate the relative performance of one propeller model compared to another especially at the climb and cruise conditions. At cruise, both the analytical predictions and test results show about a 1% advantage for the lower AF models with the more modern airfoil technology. However, as Mach number increases these analysis methods tend to over predict the measured values with the degree of over prediction increasing with increasing Mach number.

A summary showing the difference between the predicted and measured efficiency is shown in Fig. 10. The trend toward overprediction at the higher Mach numbers is easily seen in this figure. Though there appears to be more scatter at the takeoff condition the efficiency overprediction was about the same for all models at Mach 0.35, and ranged between 4 and 5%.

Investigation into the cause of this discrepancy led to the round blade shanks of the models (Fig. 7). The strip integration methods do not model the round shank as one of the

blade sections used in the calculations. The methods also do not model any potential interference losses between the blade shank and spinner, whether round or airfoil shaped. Some other tests have investigated this region of performance loss and limited empirical methods are available to estimate the interference loss also.

The effect of blade shank geometry on performance was evaluated from a number of these sources (15 to 18) and the results are shown in Fig. 11. Since some of the references had other than 3 blades, the values were chosen at the same power coefficient per blade (listed on the bottom of the figure). The results are presented in terms of the efficiency difference between airfoil shaped and "round" shank blades as a function of advance ratio. The advance ratios correspond to the three design conditions of the present test. Where possible data at the Mach numbers from the present test were used.

The first two references are propeller data where longer airfoil blade shanks were compared to round or short airfoil shanks. The third reference is data that was obtained by comparing isolated (clean) spinner measurements to spinner plus round blade stub measurements. The LeRC points are the average of the differences in performance between the predicted and measured values for all four models that were tested (from Fig. 10). The last reference is a totally empirical estimate based on the change in drag between airfoils and round blade shanks, and the change in interference drag for those shapes mounted on a flat plate. The estimated interference loss is larger than the excess drag loss associated with the isolated round blade shanks. At Mach 0.35 cruise (advance ratio of 2.234) the interference loss is about 3.4% compared to only 1.4% for the excess drag of the round shanks. The generally good agreement between the present test data and the other independent methods of evaluating blade shank losses tends to show that interference drag is the main cause of the discrepancy between the predicted and measured performance. Reducing that interference loss and the excessive drag from round shanks could improve the cruise performance of the model propellers that were tested by 4 to 5%. At higher cruise speeds these losses can be significantly higher as shown in Fig. 28 of Ref. (16). In addition, the interference and

excess blade shank drag will cause a reduction in the total pressure downstream of the shank/spinner region of the propeller that may adversely affect engine inlet recovery or cooling airflow characteristics.

The strip integration methods are currently being modified based on the results of these tests and the above loss analysis to more properly model interference and round shank losses (19). This will give these prediction methods the capability to analyze blades with either airfoil or round blade shanks. To further investigate the potential performance improvements associated with the blade shank/ spinner region, additional model tests are planned by NASA-Lewis. This future work may include contoured spinner geometries that would address a better transition shape between the spinner and blade, and could further improve G.A. propeller performance.

To evaluate G.A. acoustic prediction methods, flight tests are planned during 1981 using the Rockwell Model 690B aircraft. Full scale versions of three of the four propeller designs, that were wind tunnel tested, will be evaluated in flight to determine near and far field noise. Measured noise will be compared with acoustic predictions to improve the predictions where deficiencies are determined. Also, the same full scale propellers will be tested on the AiResearch B-26 engine test-bed aircraft, to determine relative performance characteristics and evaluate any scaling effects.

HIGH SPEED PROPELLER TESTS

In a cooperative program between NASA-Lewis and Hamilton Standard the advanced design concepts previously described in Fig. 5 for high speed turboprops were used to design a series of 62.2 cm (24.5 in) propeller models for wind tunnel testing. The most recently tested model (designated SR-6 and shown photographically in Fig. 12) was aerodynamically designed at the Lewis Research Center. The photograph shows this 69.6 cm (27.4 in) diameter model installed on the 746 kW (1000 hp) PTR in the Lewis 8-by-6 foot wind tunnel. The tunnel (20) has a porous wall test section to minimize any wall interactions. The PTR is the same rig described in earlier in this paper.

The basic blade planforms pictured in Fig. 13 represent four propeller designs that have been wind tunnel tested. The first three propellers shown in the figure (SR-2, SR-1M, and SR-3) have a blade tip speed of 244 m/sec (800 ft/sec), a cruise power loading of 301 kW/m^2 (37.5 hp/ft^2) at Mach 0.8 and 10.668 km (35 000 ft), and 8 blades. The last propeller shown in the figure (SR-6) had a design blade tip speed of 213 m/sec (700 ft/sec), a cruise power loading of 241 kW/m^2 (30 hp/ft^2), and 10 blades. The planforms are identified by sweeps of 0, 30°, 45° and 40°. Here the tip sweep is approximately the angle of the blade mid-chord at the tip of the blade measured back from a radial line normal to the axis of rotation.

The straight blade and an initial 30° swept blade (not shown) were designed using established analyses (14) that lack a refined methodology to design the twist of a swept blade. Tests of the initial 30° swept design indicated a retwist was required (which was actually a redistribution of the blade load from hub to tip). That became the 30° swept design shown in Fig. 13 (SR-1M). The 45° swept blade (SR-3) was designed for acoustic suppression as well as improved aerodynamic performance by tailoring the sweep and planform shape. The Lewis propeller design (SR-6) was based on a different design philosophy, wherein the cruise design conditions were changed from those used for the three previous propellers in order to increase predicted performance and lower noise. The design tip speed of this propeller was lowered to help reduce noise. The predicted performance lost by the lower tip speed was regained and possibly increased slightly by increasing the number of blades to 10 and lowering the power loading to 241 kW/m^2 (30 hp/ft^2). More detailed discussions of the aero/acoustic design methodology represented by the SR-3 design are presented in Refs. (21 to 23).

The efficiency and noise level that were predicted at the time these blades were designed are listed in Fig. 13 and indicate improved performance with increased sweep. The cruise noise predictions indicated some reduction for 30° of sweep and significant reduction for the aero/acoustic 45° swept design, and the 40° 10-bladed design. Experimental noise measurements on three propellers (SR-2, SR-1M, and SR-3) are reported in Refs.

(3 to 5). Relative noise levels at the blade passage tone show that SR-1m was slightly quieter than the unswept SR-2 and that the SR-3 was 5 to 6 dB quieter than SR-2. The latter significant noise reduction is in good agreement with the predicted 6 dB value in Fig. 13.

Figure 14 presents the performance of the 8-bladed propellers over the tested Mach number range. The measured net efficiencies shown in the figure are those obtained at the constant power coefficient and advance ratio corresponding to the propeller design values. These net efficiency data were extracted by cross plotting from performance data plots (similar to the low speed data from Fig. 8) for each propeller at each Mach number. Because the power coefficient and advance ratio are constant in Fig. 14, the ideal efficiency is also constant as is shown by the upper dashed line. The ideal efficiency represents the performance of a propeller with optimum loading and no blade drag. The differences between the ideal efficiency line and the experimental performance curves represent the viscous and compressibility losses. As the data curves show, those losses increase at the higher speeds due to increasing compressibility losses. However, the performance of the 45^{o} swept blade decreased a smaller amount with increasing speed than the performance of propellers with less sweep. At Mach 0.85 the 45^{o} swept blade achieved a 4% performance gain over the straight blade. The gain at Mach 0.8 was about 3%. At the lower speeds of Mach 0.6 to 0.7 both swept blades had approximately a 2 to 3% efficiency advantage over the straight blade and the highest performing design had an efficiency that exceeded 81%. The study level (shown on Fig. 14) of 79.5% efficiency at Mach 0.8, was the value used in projecting the large fuel efficiency and operating cost advantages of an advanced turboprop over an equivalent technology turbofan powered aircraft. The 45^{o} swept propeller at this speed had an efficiency of 78.7% which was close to this study level.

By operating the 45^{o} swept propeller at off design lower power loadings higher efficiencies can be obtained at Mach 0.8. This is shown in Fig. 15 where net efficiency is plotted against advance ratio for several levels of power loading. The typical variation of efficiency with advance ratio at a constant

power loading is a peaked curve. The reduction from the peak with increasing advance ratio is due to (1) a combination of lower ideal efficiencies due to increased swirl and (2) lower blade sectional lift to drag ratios (from increasing local angles of attack). The fall-off with decreasing advance ratio is due to increased compressibility losses associated with the higher tip rotational speeds and/or again lower blade section lift to drag ratios (from decreasing local angles of attack). The circle symbol in Fig. 15 represents the 45° swept propeller design point. The square symbol on the 80% power loading curve shows the design power loading and advance ratio of the 10-bladed, 40° swept propeller (SR-6). The effect of operating the 45° swept propeller at this reduced power loading and increased advance ratio (3.06 to 3.5) was to increase efficiency about 0.3%. This reduced power loading would result in a 12% larger propeller diameter in an actual aircraft installation where power requirements are fixed. Since simple geometric scaling to the larger diameter could make the aircraft hub too large, the 8-bladed, 45° swept propeller would need to be redesigned for aircraft installation to the lower hub to tip ratio of the 10-bladed, 40° swept propeller.

A comparison of the 8- and 10-bladed propellers is shown in Fig. 16 where net efficiency is plotted versus Mach number. These data show both propellers operating at the 10-bladed propeller design power coefficient and advance ratio. The performance of the 10-bladed propeller was about 3/4 to 1% higher than that of the 8-bladed model from Mach 0.6 to Mach 0.75. This higher performance was probably due to the 1% higher induced (or ideal) efficiency predicted for the 10-bladed propeller. For the 8-bladed propeller the performance loss due to compressibility effects began near Mach 0.7 and increased gradually with increasing speed. The 10- bladed propeller showed no performance loss up to speeds of Mach 0.75. Beyond this speed the efficiency fell rapidly with increasing Mach number and was about 1/2% below the 8-bladed model at Mach 0.8. This rapid performance loss is believed to be due to the onset of choking in the interblade region near the hub. This region of the propeller presented a difficult design problem because of the low hub to tip ratio and the close blade spacing.

Both of these factors would tend to reduce the interblade flow area and increase the likelihood of choking. The larger diameter increased the blade root chord and structural constraints worked against reducing the root thickness to chord ratio to provide a larger flow area. Future efforts in spinner area ruling techniques (14) to reduce the interblade root Mach number in combination with advanced cascade airfoils, and the use of lighter, structurally superior, advanced composite blade material to achieve thinner root sections may be able to alleviate these root section design problems.

FUTURE POTENTIAL

Shown in Fig. 17 are sketches of future advanced propeller concepts for both low and high speed applications. The advanced low speed propeller incorporates swept blades and proplets to improve performance and minimize noise. It would use advanced airfoils, and the blade roots would be long airfoil shapes fairing smoothly into a contoured spinner. Counter-rotation has the potential of further improving the performance of high speed propeller powered aircraft by recovering the residual swirl from single rotation propellers. The highly loaded propellers discussed earlier have about a 6% efficiency loss due to slipstream swirl. Counter-rotation has the potential for recovering most of this loss and may also reduce any blade to blade choking losses in the inboard region due to the larger spacing between blades. Both advanced single and counter-rotation propellers would be designed using the improved analysis methods that are under development by NASA (14).

Wind tunnel tests are planned by NASA to investigate both advanced lower speed and higher speed propellers. Two initial proplet propeller designs are planned for testing during 1981 in a cooperative program with Purdue University. Some of the early analytical and experimental work completed by Purdue is described in Ref. (24). In addition to the high speed propeller tests discussed earlier, NASA has plans to test at least two additional advanced single rotation models. The potential of counter-rotation is planned to be evaluated in a combined analytical and experimental program. Initial activities will include the comparison of analytical predictions, using

the counter-rotation lifting line analysis of Ref. (14) with NACA test results from the 1940's and 1950's. This will be followed by the design of a modern propeller test rig for testing advanced counter-rotation propeller models.

SYMBOLS

AF blade activity factor

$$= \frac{100\ 000}{16} \int_{\text{hub}}^{r/R=1.0} b/D(r/R)^3 d(r/R)$$

B number of blades

c elemental blade chord, cm (in.)

C_p power coefficient = $P/\rho_o n^3 D^5$

C_{Li} integrated design lift coefficient

$$= \int_{\text{hub}}^{r/R=1.0} C_{LD}(r/R)^3 d(r/R)$$

C_T thrust coefficient = $T/\rho_o n^2 D^4$

D blade tip diameter, cm (in.) or m (ft)

dB decibel

hp horsepower

J advance ratio, V_o/nD

M_o free-stream Mach number

n rotational speed, revolutions per second

P power, kW (ft-lb/sec, or hp in P/D_2 ratio)

PTR propeller test rig

R blade tip radius, cm (in.)

r radius, cm (in.)

SHP shaft horsepower

SR single rotation

T net thrust (caused by the blades only; without spinner drag or nacelle/ propeller interaction force), N (lb)

t elemental blade thickness, cm (in.)

V_o free-stream velocity, m/sec (ft/sec)

$\beta_{3/4}$ blade angle at 75% radius, deg

Δ change or difference

η net efficiency = $(T \cdot V_o)/P$

ρ_o free-stream density, kg/m^3 ($slugs/ft^3$)

REFERENCES

1. "General Aviation Propulsion," NASA CP-2126, 1980.
2. I. D. Keiter, "Impact of Advanced Propeller Technology on Aircraft/Mission Characteristics of Several General Aviation Aircraft," SAE Paper 810584, April 1981.
3. J. H. Dittmar, B. J. Blaha, and R. J. Jeracki, "Tone Noise of Three Supersonic Helical Tip Speed Propellers in a Wind Tunnel at 0.8 Mach Number," NASA TM-79046, 1978.
4. J. H. Dittmar, R. J. Jeracki, and B. J. Blaha, "Tone Noise of Three Supersonic Helical Tip Speed Propellers in a Wind Tunnel," NASA TM-79167, 1979.
5. R. J. Jeracki, D. C. Mikkelson and B. J. Blaha, "Wind Tunnel Performance of Four Energy Efficient Propellers Designed for Mach 0.8 Cruise," NASA TM-79124, 1979 or SAE Paper 790573, April 1979.
6. R. E. Neitzel, R. Hirschkron, and R. P. Johnston, "Study of Unconventional Aircraft Engines Designed for Low Energy Consumption," General Electric Co., Cincinnati, OH, December 1976. (NASA CR-135136, 1976.)
7. D. C. Mikkelson and G. A. Mitchell, "High Speed Turboprops for Executive Aircraft Potential and Recent Test Results," NASA TM 81482, 1980.

8. D. M. Black, R. W. Menthe, and H. S. Wainauski, "Aerodynamic Design and Performance Testing of an Advanced 30° Swept, Eight Bladed Propeller at Mach Numbers from 0.2 to 0.85," NASA CR-3047, 1978.
9. H. Glauert, "Wind Tunnel Interference on Wings, Bodies and Airscrews," Aeronautical Research Council, London, Reports and Memoranda No. 1566, 1933.
10. A. D. Young, "Note on the Application of the Linear Perturbation Theory to Determine the Effect of Compressibility on the Wind Tunnel Constraint on a Propeller," Aeronautical Research Council, London, Reports and Memoranda No. 2113, 1944.
11. A. J. Bocci, "A New Series of Aerofoil Sections Suitable for Aircraft Propellers," Aeronautical Quarterly, Vol. 28, February 1977, pp. 59-73.
12. S. Goldstein, "On the Vortex Theory of Screw Propellers," Proceedings of the Royal Society, London, Vol. 123, April 6, 1929, pp. 440-465.
13. T. Theodorsen, "Theory of Propellers," New York, NY: McGraw-Hill Book Co., Inc., 1948.
14. L. J. Bober, and G. A. Mitchell, "Summary of Advanced Methods for Predicting High Speed Propeller Performance," NASA TM X-81409 or AIAA Paper 80-0225, January 1980.
15. E. G. Reid, "Studies of Blade Shank Form and Pitch Distribution for Constant-Speed Propellers," NACA TN-947, 1945.
16. J. D. Maynard, "Aerodynamic Characteristics at High Speeds of Full-Scale Propellers Having Different Shank Designs," NACA RM-L6L27a, 1947.
17. J. V. Reid, "Advanced V/STOL Propeller Technology-Cruise Performance Tests." AFFDL -TR-71-88, Volume III, August 1971.
18. S. F. Hoerner, "Fluid-Dynamic Drag," Midland Park, NJ, Hoerner, S. F., 1958.
19. K. D. Korkan, G. M. Gregorek, and D. C. Mikkelson, "A Theoretical and Experimental Investigation of Propeller Performance Methodoloigies," AIAA Paper 80-1240, June 1980.
20. R. J. Swallow and R. A. Aiello, "NASA Lewis 8- by 6- Foot Supersonic Wind Tunnel," NASA TM X-71542, 1974.

21. J. F. Dugan, Jr., B. S. Gatzen, and W. M. Adamson, "Prop-Fan Propulsion - Its Status and Potential," SAE Paper 780995, November 1978.
22. F. B. Metzger and C. Rohrback, "Aero-Acoustic Design of the Prop-Fan," AIAA Paper 79-0610, March 1979.
23. D. B. Hanson, "Near Field Noise of High Tip Speed Propellers in Forward Flight," AIAA Paper 76-565, July 1976.
24. J. P. Sullivan, L. K. Chang, and C. J. Miller, "The Effect of Proplets and Bi-Blades on the Performance and Noise of Propellers," SAE Paper 810600, SAE Business Aircraft Meeting and Exposition, April 1981.

TABLE I. - LOW-SPEED PROPELLER DESIGN PARAMETERS

[All three-way propellers.]

Activity factor (per blade)	83	96	101	132
Design C_{Li}	0.42	0.40	0.55	0.53
t/c at r/R = 0.75	0.068	0.087	0.056	0.051
Airfoil type	ARA-D	GAW-2	NACA 16[a]/ Clark Y	NACA 65

[a]Tip region.

TABLE II. - LOW-SPEED PROPELLER OPERATING CONDITIONS

	Mach number	Velocity		Advance ratio, J	Power coefficient, C_p	rpm	Helical tip Mach number
		knots	m/sec				
Take-off	0.117	80	41	0.526	0.192	3064	0.708
Climb	0.224	152	78	1.103	0.204	2787	0.676
Cruise	0.35[a]	235	121	2.234	0.304	2135	0.604

[a]Tunnel limit, aircraft cruise M = 0.5.

(a) Typical lower speed aircraft, Mach 0.5 cruise.

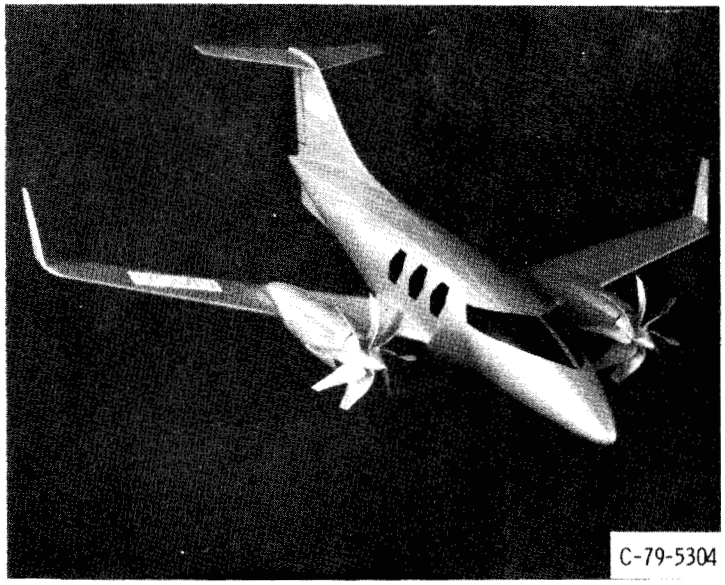

(b) Advanced high speed aircraft model, Mach 0.8 cruise.

Figure 1. - Examples of General Aviation low and high speed turboprops.

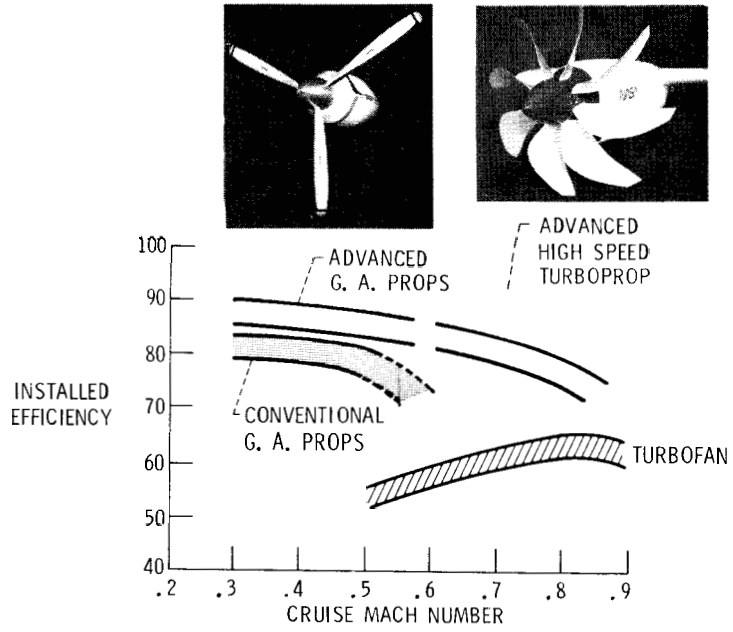

Figure 2. - Installed cruise efficiency trends.

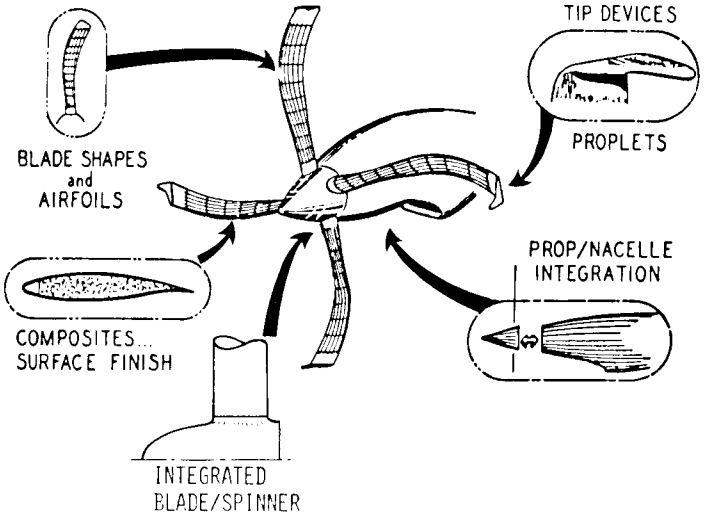

Figure 3. - Lower speed advanced technology study concepts.

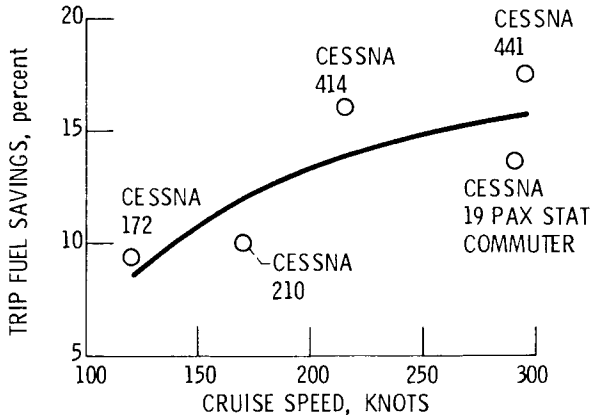

Figure 4. - Potential trip fuel savings for lower speed aircraft.

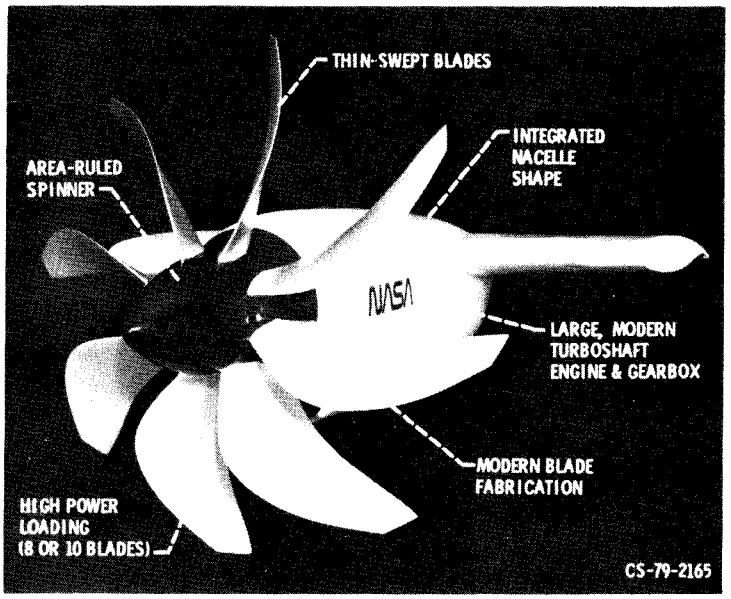

Figure 5. - Advanced high speed turboprop propulsion system.

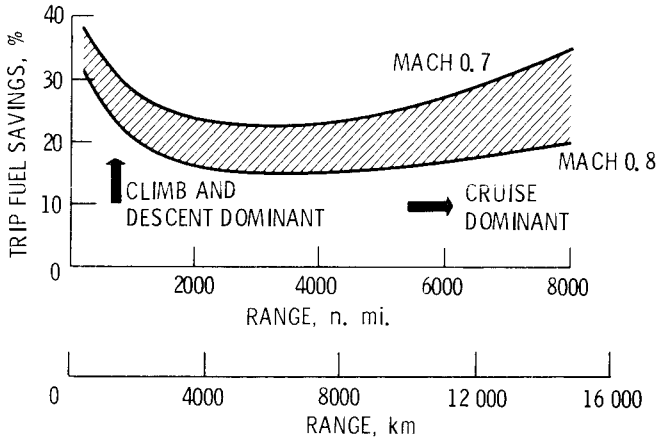

Figure 6. - Fuel savings trends of advanced higher speed turboprop aircraft over comparable turbofan aircraft.

Figure 7. - Low speed propeller model installed in the Lewis 10- by 10-Foot Wind Tunnel.

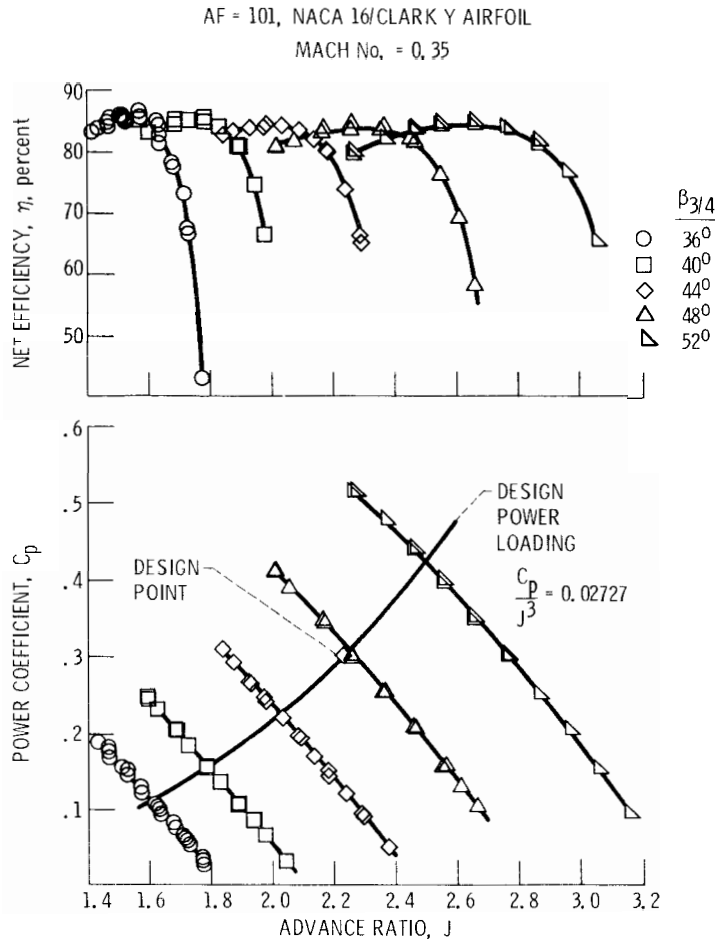

Figure 8. - Typical low speed propeller test results.

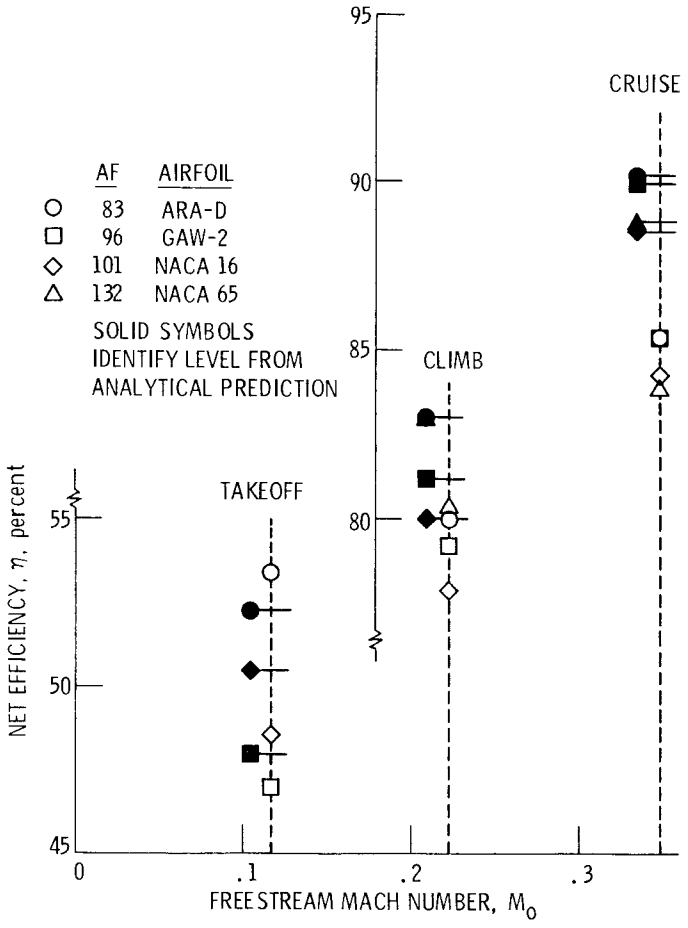

Figure 9. - Summary of low speed propeller performance.

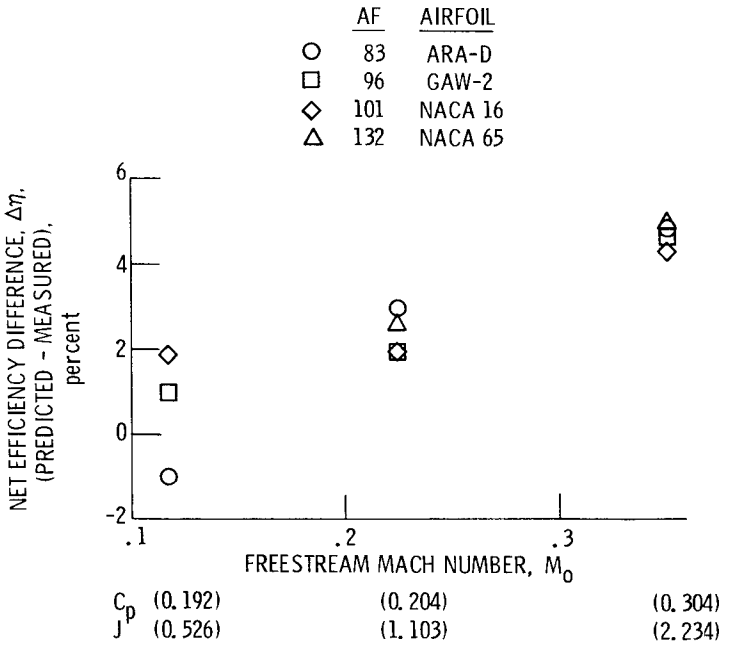

Figure 10. - Comparison of predicted and measured low speed performance.

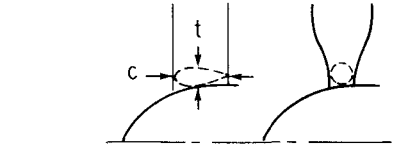

	AIRFOIL SHANK t/c	"ROUND" SHANK t/c	B #	MAX. M_0	REF.
○	.46	1.0	4	.1	15
□	.16	.6	2	.5	16
◇	—	1.0 [a]	4	.7	17
△	.3 [b]	1.0	3	.35	LeRC
▷	.45 [c]	1.0 [c]	3	—	18

a. SPINNER STUB BLADE INTERFERENCE TEST
b. PREDICTED STRIP METHOD - TEST, AVG. FIG. 17
c. EMPIRICAL LOSS ESTIMATES

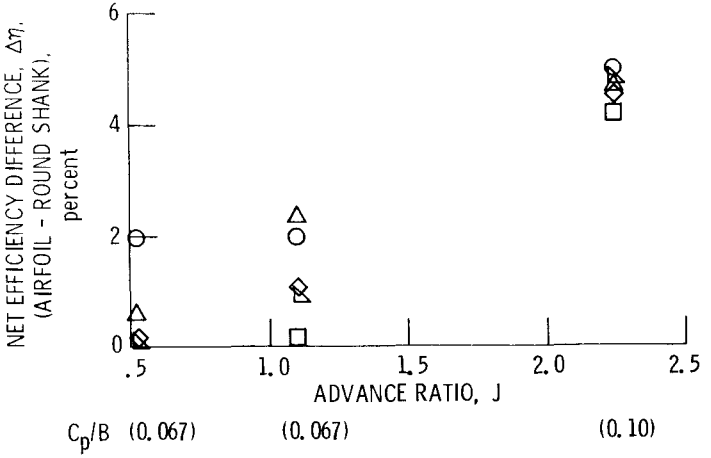

Figure 11. - Performance effect of improved blade shank design.

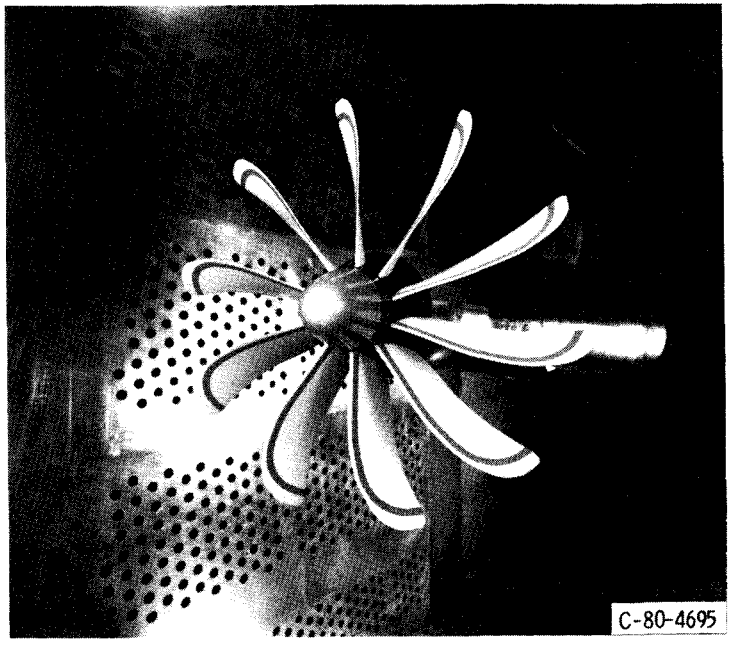

Figure 12. - High speed turboprop model installed in the Lewis 8- by 6-Foot SWT.

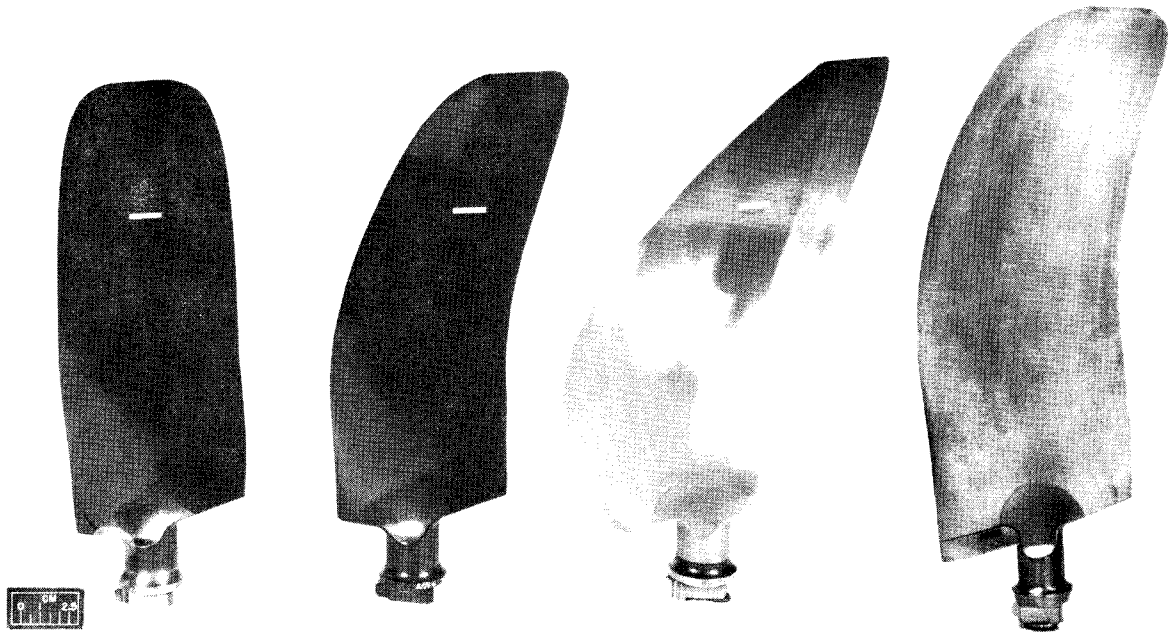

	SR-2	SR-1M	SR-3	SR-6
TIP SWEEP ANGLE, deg	0	30	45	40
PREDICTED DESIGN EFF, %	76.6	79.3	81.1	81.9
PREDICTED DESIGN NOISE REDUCTION, Δ dB	REF.	-3	-6	-6
TIP SPEED, ft/sec (m/sec)	800 (244)	→	→	700 (213)
POWER LOADING, P/D^2, hp/ft^2 (kW/m^2)	37.5 (301)	→	→	30.0 (241)
NO. OF BLADES	8	→	→	10

Figure 13. - Design characteristics and planforms of high speed propeller models.

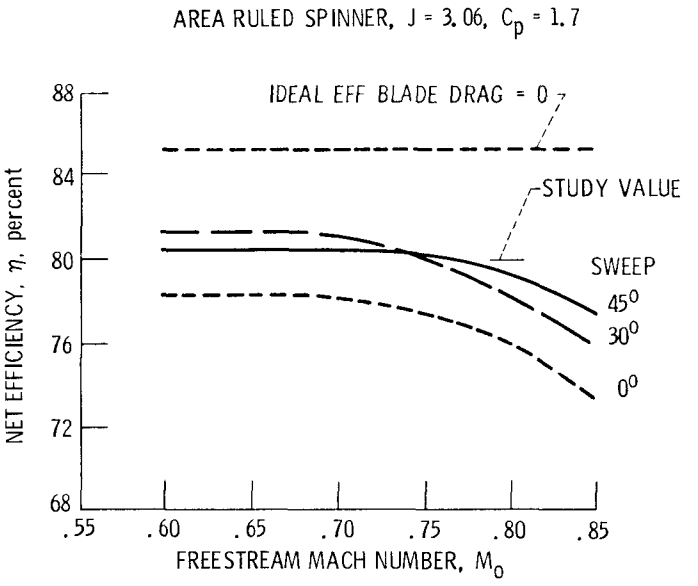

Figure 14. - High speed propeller performance summary.

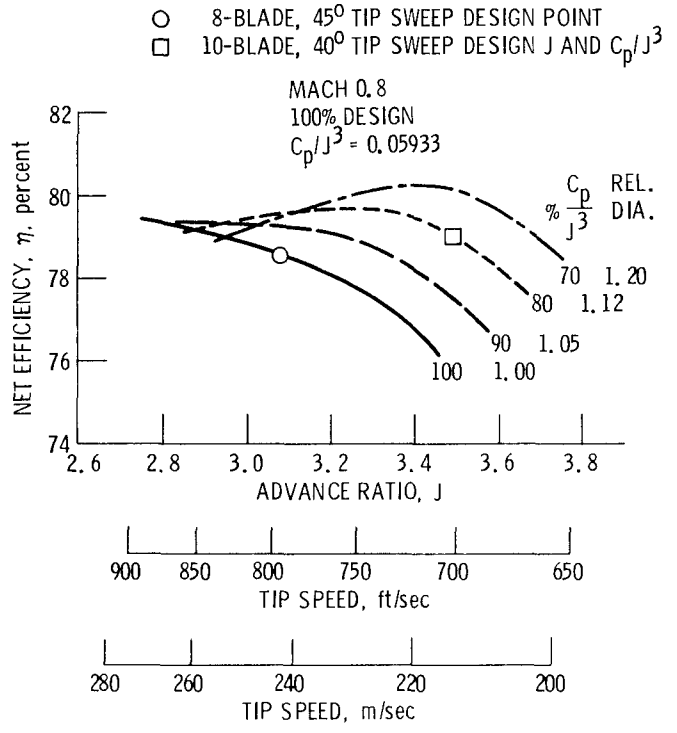

Figure 15. - Effect of power loading and advance ratio on performance of the SR-3, 45° swept propeller.

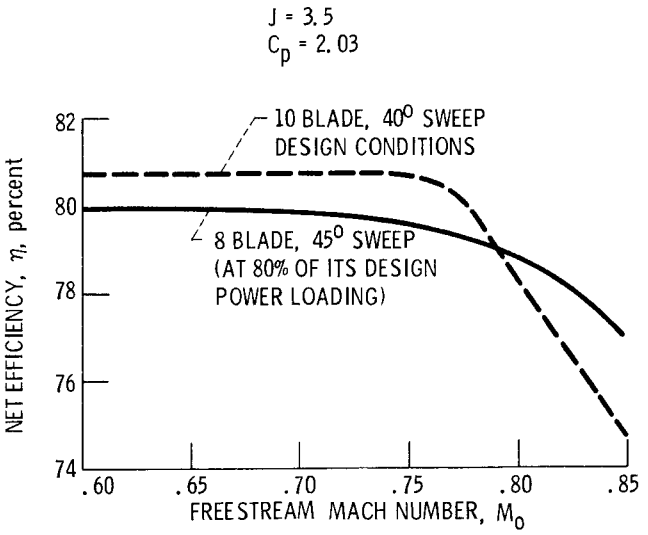

Figure 16. - Comparison of 8 and 10 blade performance.

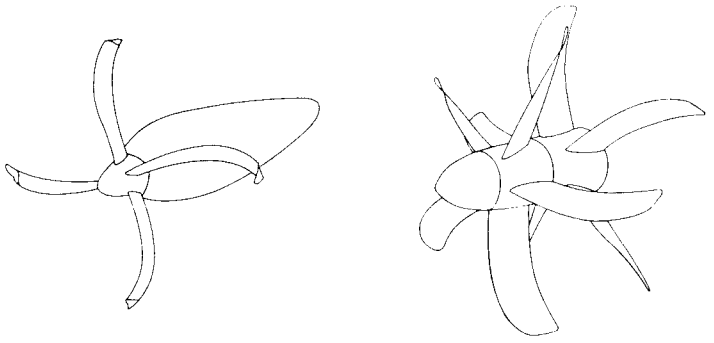

(a) Advanced lower speed.

(b) Counter-rotation high speed.

Figure 17. - Future advanced propeller concepts.

1. Report No. NASA TM-81745	2. Government Accession No.	3. Recipient's Catalog No.
4. Title and Subtitle LOW AND HIGH SPEED PROPELLERS FOR GENERAL AVIATION - PERFORMANCE POTENTIAL AND RECENT WIND TUNNEL TEST RESULTS		5. Report Date 6. Performing Organization Code 505-41-52
7. Author(s) Robert J. Jeracki and Glenn A. Mitchell		8. Performing Organization Report No. E-799 10. Work Unit No.
9. Performing Organization Name and Address National Aeronautics and Space Administration Lewis Research Center Cleveland, Ohio 44135		11. Contract or Grant No. 13. Type of Report and Period Covered Technical Memorandum
12. Sponsoring Agency Name and Address National Aeronautics and Space Administration Washington, D.C. 20546		14. Sponsoring Agency Code

15. Supplementary Notes

Prepared for the National Business Aircraft Meeting sponsored by the Society of Automotive Engineers, Wichita, Kansas, April 7-10, 1981.

16. Abstract

Research sponsored by NASA has indicated that there is a significant potential for improving the performance of propellers designed for general aviation (G.A.) aircraft that cruise at speeds below about Mach 0.6. At higher cruise speeds (Mach 0.6 to 0.8) the turbofan powered business aircraft has been dominant. However, research underway at NASA has also indicated that there is a large potential performance gain and fuel savings for future aircraft powered by advanced turboprop propulsion. To evaluate the performance of current technology lower speed G.A. propellers, four 5-foot diameter models were recently tested in the Lewis 10×10 foot wind tunnel. These three-way models had variations in the level of airfoil technology and activity factor. At cruise, the measured performance was about 4 to 5% below the level predicted by existing analytical procedures. A large part of this difference appears to be associated with inadequate modeling of blade and spinner losses for propellers round shank blade designs. In future propeller designs, incorporation of blade cuffs and shaping of the spinner/blade junction may offer the potential of recovering most of these losses. The performance of this category of G.A. propellers may be further improved by incorporating advanced concepts that are currently being investigated. These concepts include: advanced blade shapes (airfoils and sweep), tip devices (proplets), integrated propeller/nacelles, and composites. The potential improvements associated with these concepts may result in a 10 to 15% reduction in trip fuel for future lower speed G.A. aircraft. To achieve high performance with turboprop powered aircraft that cruise at higher speeds, propeller compressibility losses will have to be minimized or eliminated, and power loading (SHP/D^2) will have to be increased considerably. Several advanced aerodynamic concepts, that have the potential for improving propeller performance at high cruise speeds, were evaluated in the Lewis 8×6 foot wind tunnel. Five 2-foot diameter propeller models were tested to investigate: increased blade number (8 and 10 blades), reduced blade thickness, blade speed, spinner area ruling, and integrated propeller/nacelles. Results from these tests show that high propeller performance can be obtained to at least Mach 0.8. At this speed an advanced turroprop has the potential of reducing trip fuel by 15 to 30% compared to equivalent technology high bypass ratio turbofans.

17. Key Words (Suggested by Author(s)) Fuel conservation Advanced turboprop Propeller General aviation	18. Distribution Statement Unclassified - unlimited STAR Category 02		
19. Security Classif. (of this report) Unclassified	20. Security Classif. (of this page) Unclassified	21. No. of Pages	22. Price*

* For sale by the National Technical Information Service, Springfield, Virginia 22161